

Manuscript 1470

A case study comparing the results of a copper open-pit mine scheduling considering two different approaches for spatial interpolation of comminution geometallurgical variables

Author(s) ORCID Identifier:

Sílvia de Castro Martins:  0009-0001-3077-0263

Pedro Campos:  0000-0001-5208-7177

Douglas Mazzinghy:  0000-0003-2569-6932

Follow this and additional works at: <https://jism.gig.eu/journal-of-sustainable-mining>

 Part of the [Explosives Engineering Commons](#), [Oil, Gas, and Energy Commons](#), and the [Sustainability Commons](#)

A case study comparing the results of a copper open-pit mine scheduling considering two different approaches for spatial interpolation of comminution geometallurgical variables

Abstract

The use of geometallurgical variables to improve the accuracy obtained in mine planning is an increasingly present reality in mining. However, the way these variables are interpolated to construct the block model is still a major challenge since they are non-additive variables. In this case study, a database from a copper mine located in Brazil was used to compare mining planning by Direct Block Scheduling using two spatial interpolation approaches. In the first approach, the geometallurgy block model was produced interpolating the comminution indexes A_{xb} and BWI from the drill holes, and the specific energy was calculated at each block. The second approach consisted of calculating the specific energy at the drill holes first, then interpolating the values into the blocks. The results indicated that the difference between the two approaches was not significant. Both block models produced a mine life equal to seven years and a percentage difference in the accumulated NPV of 0.54%.

Keywords

geometallurgical variables, non-additive variables, Direct Block Scheduling, comminution indexes.

Creative Commons License



This work is licensed under a [Creative Commons Attribution-Noncommercial-No Derivative Works 4.0 License](https://creativecommons.org/licenses/by-nc-nd/4.0/).

A case study comparing the results of a copper open-pit mine scheduling considering two different approaches for spatial interpolation of comminution geometallurgical variables

Sílvia Martins^{a,b,*} , Pedro Campos^a , Douglas Mazzinghy^a 

^a Federal University of Minas Gerais, Graduate Program in Metallurgical, Materials and Mining Engineering (PPGEM), Brazil

^b Federal Center of Technological Education, Brazil

Abstract

The use of geometallurgical variables to improve the accuracy obtained in mine planning is an increasingly present reality in mining. However, the way these variables are interpolated to construct the block model is still a major challenge since they are non-additive variables. In this case study, a database from a copper mine located in Brazil was used to compare mining planning by Direct Block Scheduling using two spatial interpolation approaches. In the first approach, the geometallurgy block model was produced interpolating the comminution indexes Axb and BWI from the drill holes, and the specific energy was calculated at each block. The second approach consisted of calculating the specific energy at the drill holes first, then interpolating the values into the blocks. The results indicated that the difference between the two approaches was not significant. Both block models produced a mine life equal to seven years and a percentage difference in the accumulated NPV of 0.54%.

Keywords: Geometallurgical variables, Non-additive variables, Direct block scheduling, Comminution indexes

1. Introduction

Geometallurgy is a multidisciplinary approach that combines geological and mineralogical information with mineral processing, being able to predict the metallurgical response of different ore lithologies. Its greatest application is in mineral deposits that have high variability between different lithologies. Its purpose is to predict the processing capacity of each lithology and, consequently, the mine capacity with greater precision. Therefore, this information can be used during the mine planning stage to optimize results, making them more accurate and providing greater resilience to the mining project [1–3]. Many authors present in their research the use of geometallurgical variables as a way to reduce risks and increase project precision [4–9].

Despite the advantages associated with geometallurgy, the use of this tool is still incipient, and

many uncertainties exist regarding the use of geometallurgical variables. Geometallurgical variables are classified into primaries and responses [10]. The primary variables are inherent to the properties of the ore, for example, in situ density and grades, and can be measured directly in the rock. The response variables correspond to the attributes of the ore that describe the metallurgical responses during processing, such as recovery in flotation or the performance of the ore in the comminution plant. To measure them, it is necessary to carry out bench-scale tests of flotation or leaching in the case of metallurgical recovery, and comminution tests like BWI [11], DWT [12], SMC [13], for example.

Metallurgical recovery can be defined as the mass of useful element or metal present in the feed that is sent to the concentrate during the mineral concentration process. Metallurgical recovery depends mainly on the lithology of the ores and metal grade [14].

Received 21 May 2024; revised 7 December 2024; accepted 12 December 2024.
Available online 1 October 2025

* Corresponding author.
E-mail address: silviaengminas@cefetmg.br (S. Martins).

<https://doi.org/10.46873/2300-3960.1470>

2300-3960/© Central Mining Institute, Katowice, Poland. This is an open-access article under the CC-BY 4.0 license (<https://creativecommons.org/licenses/by/4.0/>).

However, a common practice when carrying out mine planning is to consider that the different materials feeding the concentration plant will have the same metallurgical recovery. This simplification will imply a mass of metal obtained after the concentration process distinct from the mass predicted in the planning stage, impacting the mine’s financial return [15].

Another simplification made in traditional mine planning is disregarding each block’s performance in the comminution stage. Depending on the block hardness, it may need a certain time in the comminution circuit to obtain the desired particle size for subsequent steps. In other words, a block with high hardness with higher specific energy will take longer to reach a certain particle size than a block with lower specific energy. This will directly impact the plant’s throughput and, consequently, the metal rate produced [16,17].

The modeling of geometallurgical variables is a complex task as it usually involves non-additive variables. A variable is additive when there is a linear averaging of values, that is, combinations between samples produce results consistent with the weighted average. A variable is non-additive when there is no linear averaging between two equal characteristics [18–21].

Table 1 presents the study carried out with two lithologies, BTOS and QSRT, from the Chapada Mine (Lundin Mining), where the non-additive character of the Axb and BWI variables is demonstrated [22].

As seen in Table 1, the blending of these blocks will result in a sample with density-weighted by the volume, however, the value of Axb and BWI will not necessarily correspond to the average since Axb and BWI is a non-additive variable. In fact, mixing the two samples would result in the Axb and BWI closest to the Axb and BWI of sample 2. This is because the lithology that is more resistant to breakage tends to accumulate inside the mill during the BWI test [20,23].

The same happens when spatial interpolating geometallurgical variables to assemble the block model. Consider the block model shown in Figure 1 as an example. In Figure 1a, the three-dimensional

Abbreviations	
BWI	Bond Work Index
SMC	Steve Morell Comminution
DBS	Direct Block Scheduling
DWT	Drop Weight Tester
HIT	Hardness Index Tester
NPV	Net Present Value
IDW	Inverse Distance Weighting

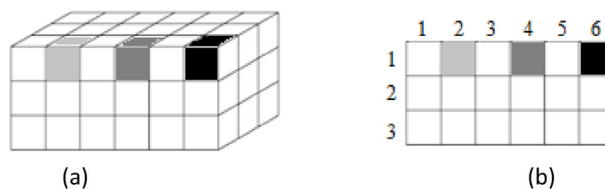


Fig. 1. (a) Three-dimensional block model. (b) Section taken from the three-dimensional model (Source: created by the authors).

model is shown, while in Figure 1b, a section of the block model was taken.

In the section (Fig. 1b), there are three blocks from line 1 highlighted. The block in column 2 and column 6 contains information that was estimated from drill holes that intersected the block. Other blocks have their information obtained from interpolation between blocks 2 and 6. If block 2 is made up of a rock with a lower BWI and block 6 is made up of a rock with a higher BWI, the spatial interpolation for block 4 would generate an average value between blocks 2 and 6. However, this value may not be the best estimate since BWI is a non-additive variable. However, it is the practice of the mining industry to interpolate them using linear methods, such as kriging and inverse distance weighting (IDW).

Even though the comminution indexes are non-additive variables, the specific energy calculated from these indexes is considered an additive variable when based on the mass of these blocks [24]. In general, any parameter that is a relationship between variables, if it is additive, will only be so if the weighting is by the same unit of the parameter denominator variable [25].

The main objective of this research was to evaluate the results obtained in the mine planning of an open-pit copper and gold mine using two different spatial interpolation approaches. In the first approach, the comminution indexes Axb and BWI present in the drill holes were spatially interpolated using IDW (power 3) for subsequent calculation of the specific energy of each block. In the second approach, the specific energy in the drill holes was first calculated and then spatially interpolated using the IDW (power 3). The interpolation method was

Table 1. Axb, BWI, and density results for the evaluated mixtures.

Sample	% BTOS	% QSRT	Axb	BWI	Density
01	100	0	135.51	6.95	2.76
02	0	100	70.34	11.31	2.69
03	50	50	92.61	10.52	2.72
Calculated weighted average	50	50	73.41	9.31	2.72

Source: Adapted from [22].

not the object of study in this research; therefore, comparisons of different interpolation methods on comminution indexes and specific energy were not carried out. IDW interpolation was used because it is the method currently used by the company. As a secondary objective, this work shows how to obtain comminution indices from HIT, a fast, low-cost test that is easily reproducible in other mines, and how to apply them in mine planning. No similar works were found in the relevant literature.

2. Materials and methods

2.1. Database

The data used in this research comes from a Brazilian copper and gold mine and, for reasons of secrecy, the name will not be revealed. The company currently has different pits in operation, and one of them was selected to be used in the research.

The pit selected has 2,489,810 blocks, 82,601 of which are mineralized; each block has dimensions of $10 \times 10 \times 10$ m, and 113 drill hole samples with HIT test results (Axb and BWI) [26–29] and 12 drill hole samples with DWT [12] and BWI [11] test results. Figures 2 and 3 show the distribution of copper and gold grades of the mineralized blocks in the studied pit, respectively. The mine has a total of ten pits, and the plant is fed by a blend of equal proportions from three simultaneous pits. As only one pit was used in this research, process capacity values input as parameters in mine planning, as well as the installed power of the comminution, were proportional to the participation of the pit under study.

2.2. Metallurgical recovery calculations

Metallurgical recoveries of copper and gold are calculated by the company depending on lithology and feed grades. The copper and gold recovery

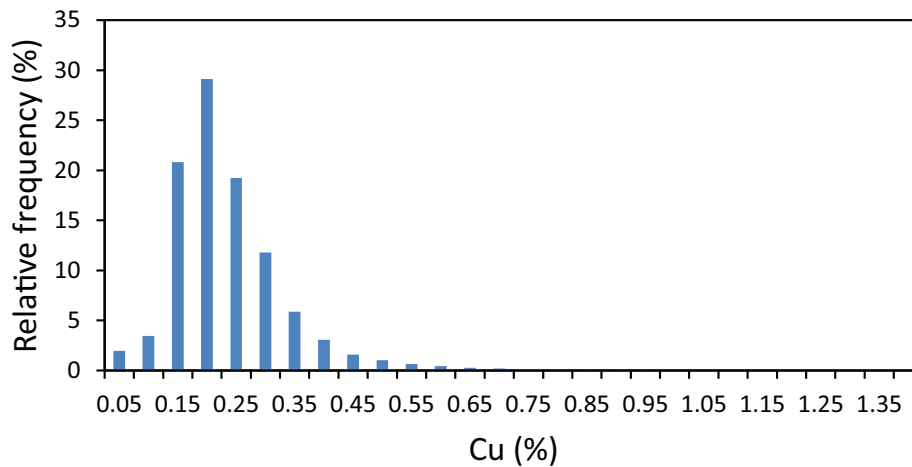


Fig. 2. Histogram of Cu grades (Source: created by the authors).

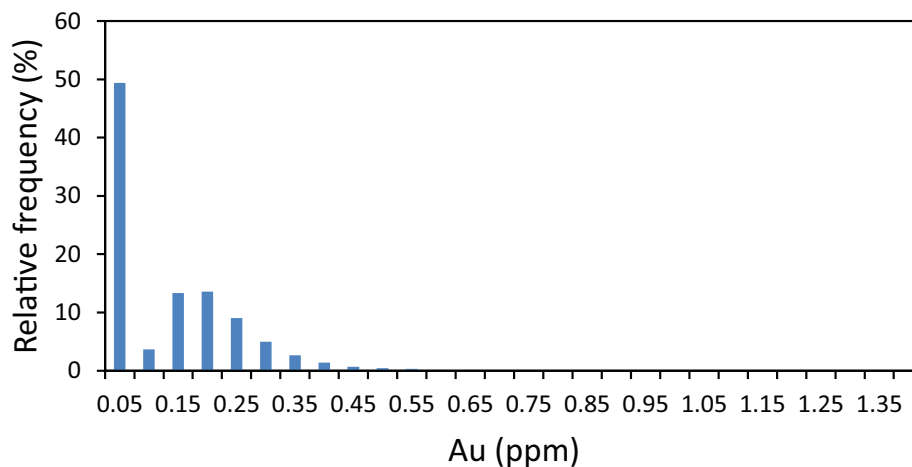


Fig. 3. Histogram of Au grades (Source: created by the authors).

equations are shown in Table 2 and Table 3, respectively.

2.3. Block specific energy calculations

The geometallurgical data provided by the company involved the comminution indices Axb and BWI , obtained mostly from the HIT. The HIT is a simplification of the DWT, which is also used by the mining company to obtain the Axb parameter.

In DWT, mineral particles are separated into three batches based on their particle size and are subjected to different impact levels with a determined energy. After the particles in each batch are broken, the particle size analysis of the fragments generated is performed. As a result, this test will provide the Axb comminution index. However, it is a costly test, requiring 50 kg of samples that will be destroyed in the test, which may make it unfeasible to use it on a large scale to obtain geometallurgical data.

The alternative used by the mining company to determine comminution performance is the HIT. With a design similar to the equipment used in the DWT, the HIT can quickly and cheaply estimate the $A*b$ comminution parameters directly and the BWI through calibration. The test is performed in less than 10 minutes, using less than 500 g of fragments, and can be performed in the mine itself, without the need to send samples to a laboratory. Comminution indices are calculated using online software [30]. This test is not a replacement for standard comminution tests, but it is capable of generating a high number of comminution indices, significantly reducing the need for standard laboratory testing [31].

Total energy was calculated according to Equation (1), which is part of the methodology proposed by

Steve Morrell in his SMC test [13]. The SMC test can be considered a simplification of the DWT. With a similar design, the SMC test uses 15–20 kg of samples.

$$E_t = 4Mia \left(750^{-\left(0.295+750/10^6\right)} - F_{80}^{-\left(0.295+F_{80}/10^6\right)} \right) K_1 + 4Mib \left(P_{80}^{-\left(0.295+P_{80}/10^6\right)} - 750^{-\left(0.295+750/10^6\right)} \right) \tag{1}$$

where: Mia : working index of the coarse ore fraction; F_{80} : 80% passing in the feed of the grinding circuit (μm); K_1 : pebble mill efficiency factor, being 0.95 when there is pebble recirculation and 1 when there is no pebble recirculation; Mib : work index of the fine ore fraction, in this case, Mib_{target} ; P_{80} : 80% passing in the product of the grinding circuit (μm).

The parameters used in Equation (1), Mia and Mib , are calculated from an extensive closed database, fed back by samples sent to licensed laboratories. The calculation procedures for obtaining these parameters are confidential, which prevents their exact reproduction [11]. Despite this, there are equations that tend to estimate these parameters. The parameters Mia and Mib were estimated using the equations presented by Refs. [32,33], shown in Figures 4 and 5, respectively.

In Figure 5, the P_{100} equation at 150 μm was used, which was the control grid used in the BWI test and is equivalent to a P_{80} of 114 μm . However, the mine operates with a P_{80} of 280 μm . Therefore, Equation (2) was used to determine the Mib of the plant [13].

$$Mib_{\text{target}} = Mib_{\text{ref}} \left(\frac{P_{80\text{ref}}}{P_{80\text{target}}} \right)^{0.24} \tag{2}$$

where: Mib_{target} : Mib in the calculation that is required to be carried out; Mib_{ref} : Mib obtained using the data from the Bond laboratory ball work index; $P_{80\text{target}}$: P_{80} in the calculation that is required

Table 2. Copper recovery equation.

Recovery Cu	Lithology	a	b
$a \cdot \ln(\text{Cu feed grade}) + b + 1.5$	A	13.626	99.487
	B	11.411	95.172
	C	9.080	90.357
	D	11.799	96.158
	E	11.479	89.862

(Source: data provided by the mining company)

Table 3. Gold recovery equation.

Recovery Au	Lithology	a	b
$a \cdot \ln(\text{Au feed grade}) + b$	A	13.948	79.787
	B	12.529	73.521
	C	11.791	68.321
	D	10.099	65.882
	E	12.092	67.474

(Source: data provided by the mining company)

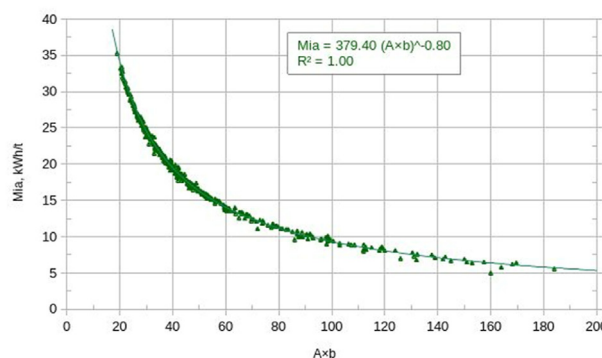


Fig. 4. Relationship between Mia and Axb (Source: [32]).

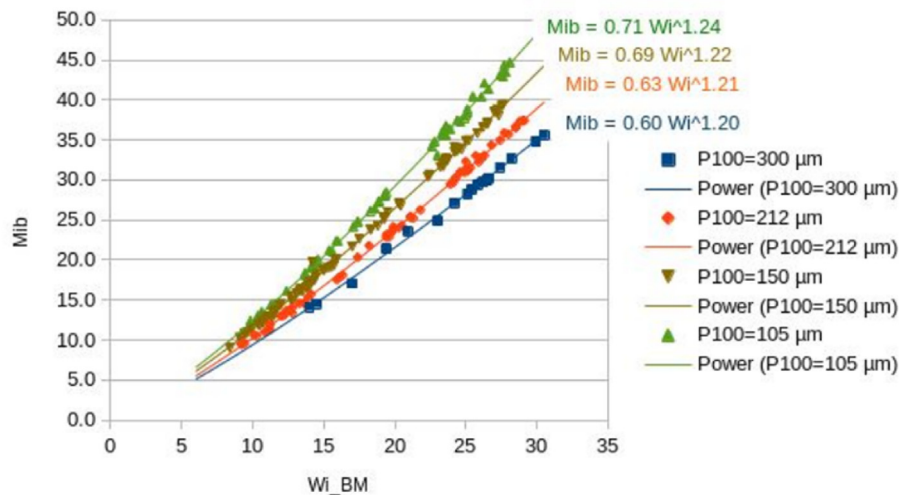


Fig. 5. Relationship between Mib and BWI (Source: [33]).

to be carried out; P_{80ref} : P_{80} obtained in the Bond laboratory ball work index test.

To calculate the Mia and Mib values were used F_{80} of 146,000 μm , K_1 of 0.95 and P_{80} of 280 μm .

Finally, the throughput of each block during grinding was calculated according to Equation (3), and the comminution time of the block according to Equation (4).

$$TPH = \frac{P}{E_t} \quad (3)$$

$$P_h = \frac{TPH}{M_B} \quad (4)$$

where: TPH : throughput (t/h); P : installed power of the comminution plant (W); E_t : specific energy (kWh/t); P_h : process hours; M_B : mass of the block (t).

2.4. First approach: interpolating the BWI and A_{xb} comminution indexes

Using the company's block model, with the comminution indexes A_{xb} and BWI interpolated through IDW (power = 3), the specific energy, throughput and metallurgical recovery of each block were calculated. Using this block model, mine planning was carried out by DBS. Figure 6 shows the diagram of the steps performed.

2.5. Second approach: interpolating the specific energy

Following the SMC methodology [13], the total specific energy was calculated based on the results of the HIT (A^*b and BWI). The specific energy was interpolated using the IDW (power = 3). Finally, the

specific energy, throughput and metallurgical recovery of each block were calculated. Using this block model, mine planning was carried out by DBS. Figure 7 shows the diagram of the steps performed.

2.6. Direct Block Scheduling (DBS)

Mine scheduling was carried out using Mining-Math software [34] that uses DBS in optimization [35,36].

The geometallurgical variables were inserted directly into the block model provided by the company. The metallurgical recovery of each block was calculated according to the equations provided in Tables 2 and 3. The specific energy was calculated according to Equation (1), and the comminution time for each block was calculated from this, according to Equation (4). In addition, two columns were included in the block model, one to calculate the value of the block if it is ore and the other to calculate if it is waste, according to Equations (5) and (6).

$$BEV_o = \left[M_B \cdot \left(\frac{g_{Cu}}{100} \right) R_{Cu} \cdot (P_{Cu} - C_{Cu}) + \left(M_B \cdot g_{Au} \cdot R_{Au} \cdot (P_{Au} - C_{Au}) \right) \right] - [M_B \cdot (C_P + C_M)] \quad (5)$$

$$BEV_w = -M_B \cdot C_M \quad (6)$$

where: M_B : block mass (t); R_{Cu} and R_{Au} : a general term that involves the recovery in the concentration and refining of copper and gold, respectively; P_{Cu} and P_{Au} : selling prices for copper (\$/t) and gold (\$/g), respectively; C_{Cu} and C_{Au} : are costs arising from the

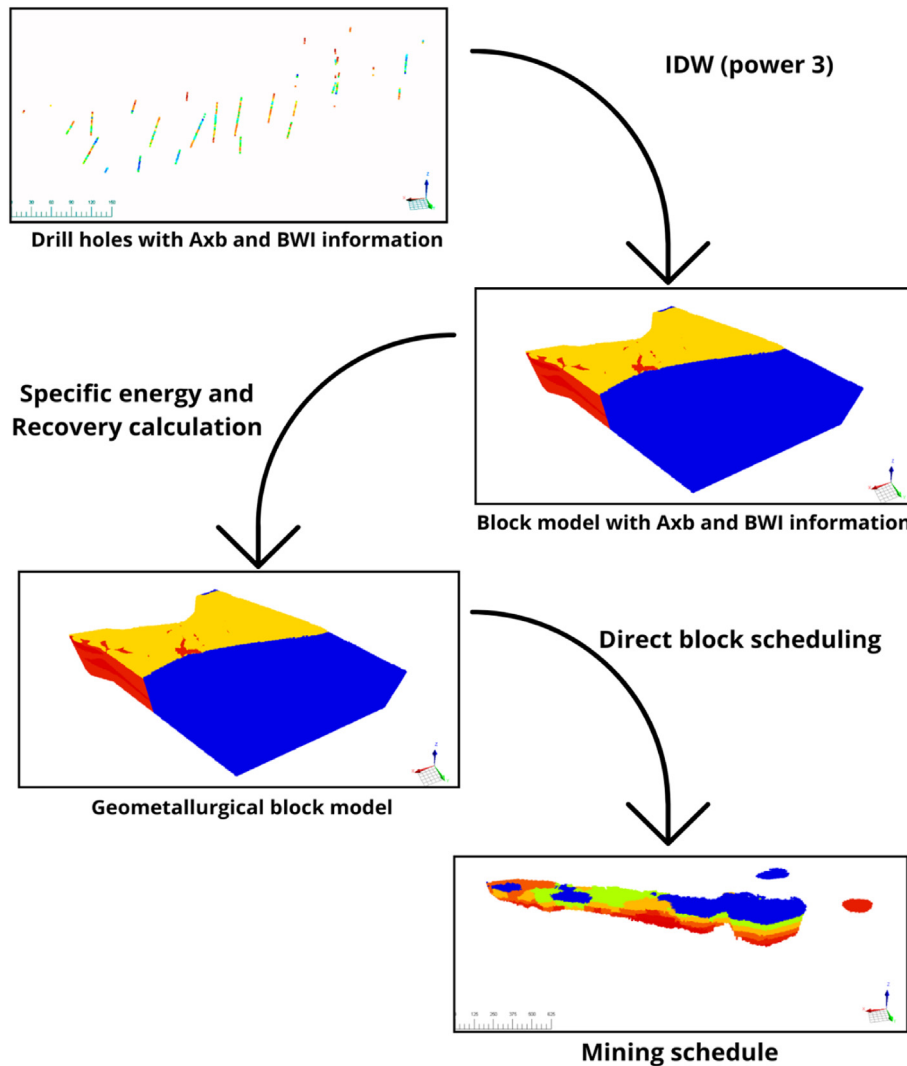


Fig. 6. Diagram of the first approach (Source: created by the authors).

product and commercialization stages, such as smelting, refining, packaging, freight, copper and gold insurance; C_P : processing cost; C_M : mine cost.

The costs and sales prices used in Equations (5) and (6) were taken from the mining company's Technical Report and are presented in Table 4.

This was the dataset fed into MiningMath. To configure the optimization in the software, the data on capacities, mining geometries, grade restrictions and discount rate were filled in. These parameters used during the optimization, as well as the mine and process capacities, were provided by the company and are presented in Table 5.

In addition, it was indicated which columns of the dataset the software should search for to perform the optimization. The comminution time column that was created in the dataset is indicated as a sum variable within the software, being limited to the

annual operating time of the plant (8060 h). This means that the processing time of each block sent to the plant in a given year will be added up. When this sum reaches 8060 h, it is no longer possible to send blocks to the plant, even if its annual capacity has not been reached.

3. Results and discussion

3.1. Statistical analysis

Figures 8 and 9 present the specific energy histograms of the blocks in the first and second approaches, respectively.

The block model in the second approach presented a greater number of blocks with higher energy (above 11 kWh/t), reaching a maximum value of 15.78 kWh/t, against 14.57 kWh/t in the first

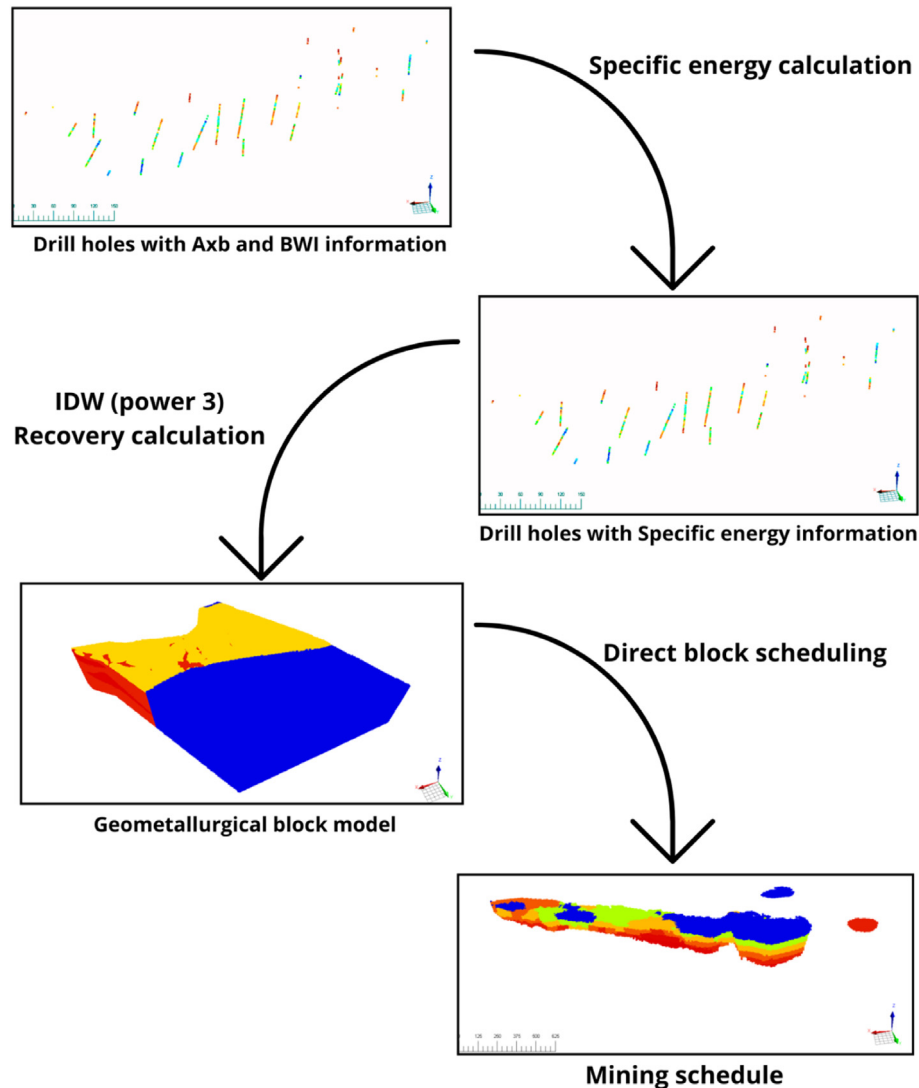


Fig. 7. Diagram of the second approach (Source: created by the authors).

Table 4. Economic parameters.

Parameters	Values
Selling price Cu	8,818.48 US\$/t
Selling price Au	51.45 US\$/t
Selling cost Cu	1388,91 US\$/t
Selling cost Au	0.14 US\$/t
Mine cost	4.79 US\$/t
Processing cost	3.31 US\$/t

(Source: Technical Report)

Table 5. Input parameters for DBS optimization.

Parameters	Values
Annual discount rate	18%
Process capacity	8 Mt/year
Total mine capacity	24 Mt/year
Minimum mine width	10 m
Minimum pit bottom size	30 m
Minimum mine length	50 m
Annual average copper grade	0.1 a 0.4%
Total operating hours of the plant	8060 h/year

(Source: data provided by the mining company)

approach. This means that the block model in the first approach underestimated the specific energy of the blocks.

3.2. DBS

DBS optimization returned seven years of life of Mine (LoM) for both block models. The difference in block extraction can be seen in the images shown in Figure 10a and b.

Figure 10 shows that the mine scheduling results were different in the two approaches, even though, in general, the removal of blocks was carried out in similar regions, resulting in similar final pits. This result may seem strange at first since the difference between the block models used in each approach is only in the block processing time. Analyzing Figure 11, it is possible to understand the reasons for this difference. This figure shows what would

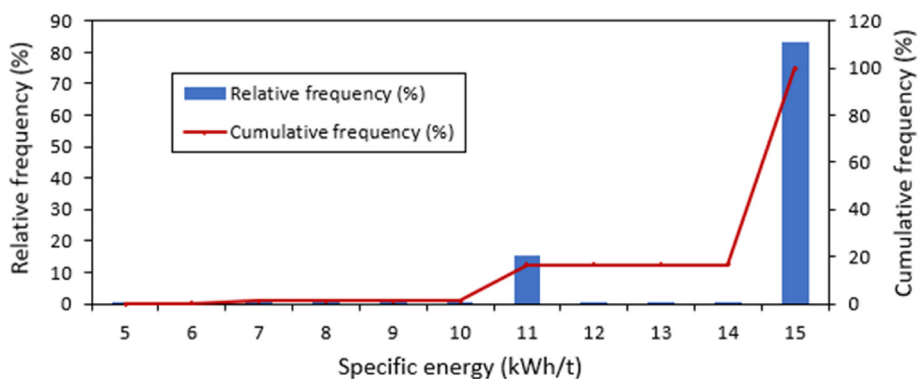


Fig. 8. Histogram of the specific energy of the blocks in the first approach (interpolation of BWI and Axb) (Source: created by the authors).

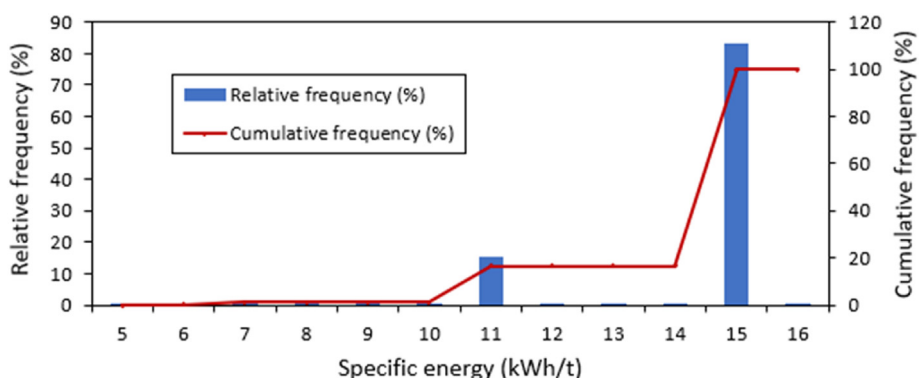


Fig. 9. Histogram of the specific energy of the blocks in the second approach (Interpolation of specific energy) (Source: created by the authors).

happen to the plant’s annual processing time if the block model of the second approach (Interpolation of specific energy) had the same mine scheduling used in the block model of the first approach (Interpolation of BWI and Axb).

As expected, the block model of the first approach (Interpolation of BWI and Axb) did not exceed the processing time of 8060 hours, which was a constraint inserted in the mine scheduling. However, extracting the same sequence of blocks in the block model of the second approach (Interpolation of specific energy), it is noted that in the first period there were not enough blocks extracted to reach the plant’s operating time limit. This indicates that the sum of blocks mined during the first period in the model used in the second approach (Interpolation of specific energy) is smaller than the sum of blocks mined in the model of the first approach (Interpolation of BWI and Axb).

From the third year onwards, the processing time of the blocks in the model of the second approach (Interpolation of specific energy) is greater than that of the blocks present in the first approach (Interpolation of BWI and Axb), causing the sum of the

processing time of these blocks to exceed the plant’s operating time limit. Therefore, even if the economic value of the blocks is the same in the models used in both approaches, it would be impossible for the software to generate two identical block schedules due to plant operating time constraints. Then, the mine scheduling optimization software scheduled the two approaches differently in order to meet the plant’s operating time constraints.

The results presented for the two block schedules shown in Figure 10 will be presented in Figure 12 which shows the mass sent for processing in both approaches.

As can be seen in Figure 12, the masses sent for processing were very similar from period to period, differing by a maximum of 0.70 Mt in the 3rd year. The mass of blocks processed in the first approach (Interpolation of BWI and Axb) throughout the life of the mine was 43.25 Mt and in the second approach (interpolation of specific energy), 42.90 Mt. However, the production of 8 Mt tons is not achieved in either approach. Since the geometallurgical approach considers the specific energy of each block, the processing time of these blocks becomes a

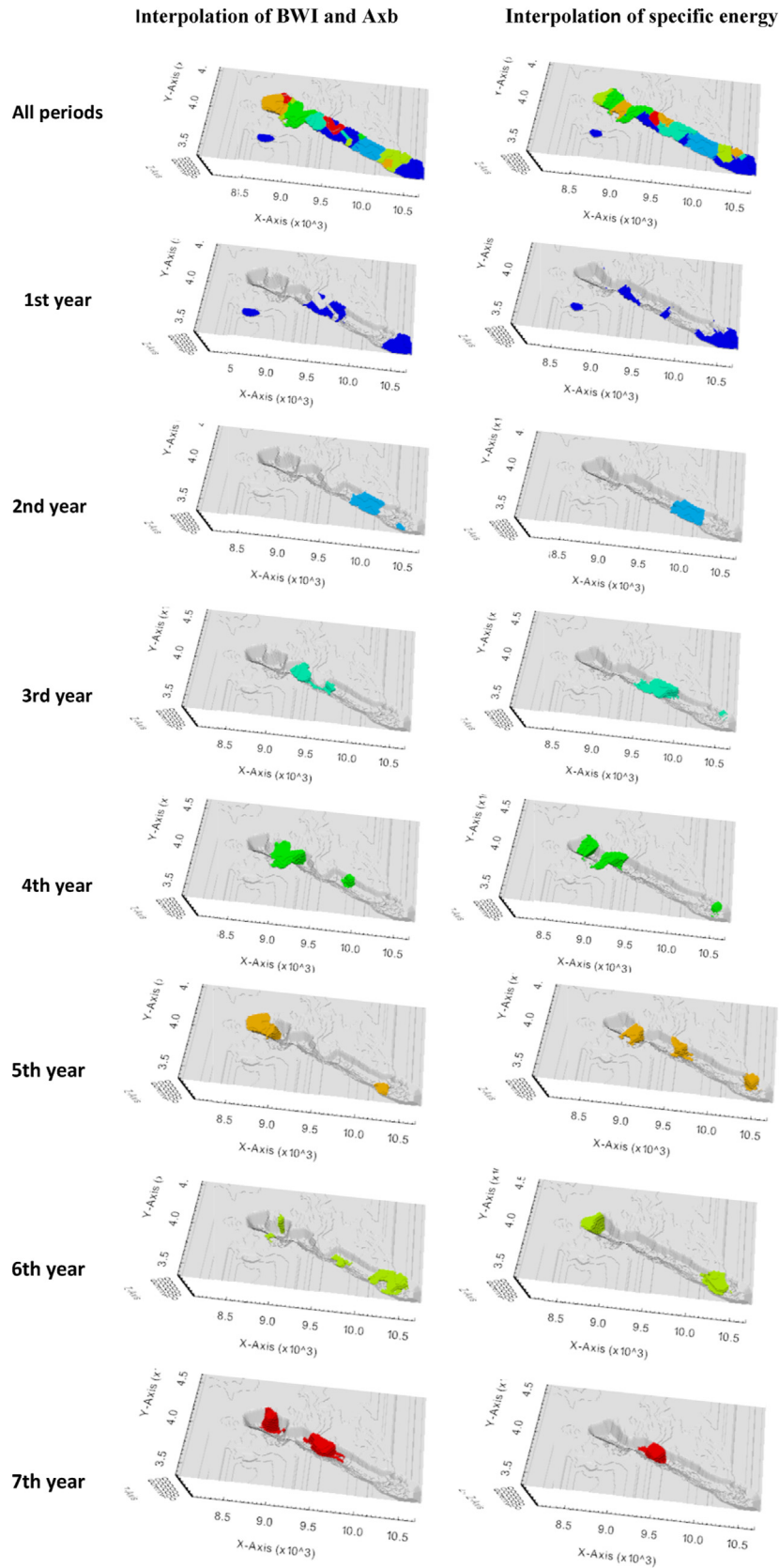


Fig. 10. Extraction sequence period by period and all periods (Source: MiningMath).

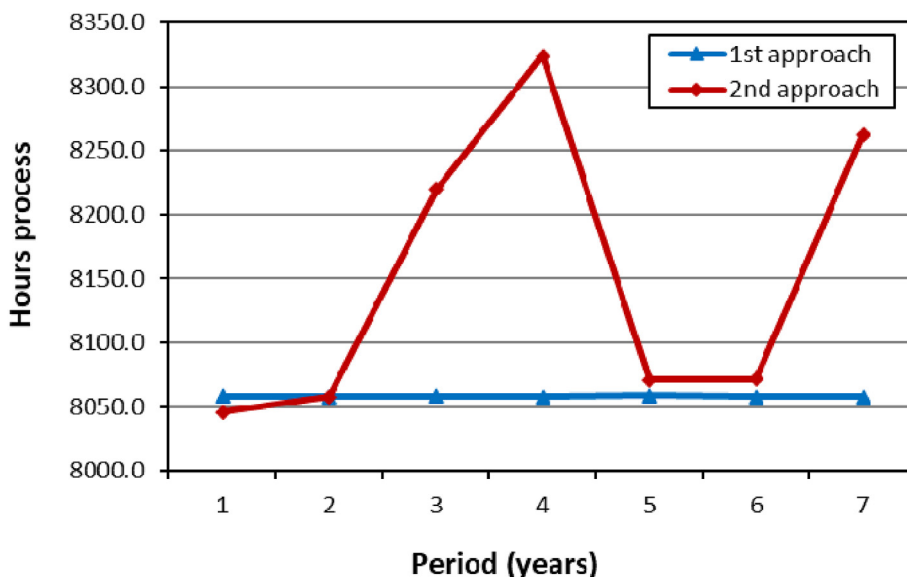


Fig. 11. Annual processing time for the block models of the 1st and 2nd approaches when the blocks are extracted according to the scheduling obtained in the 1st approach (Source: MiningMath).

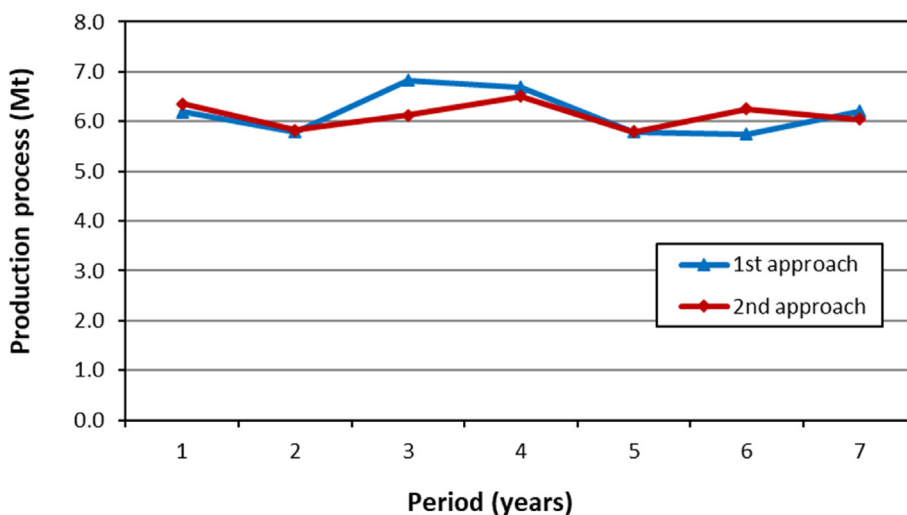


Fig. 12. Production process period by period in both approaches (Source: MiningMath).

bottleneck, interfering with the plant’s production. This is due to the annual processing time of 8060 h, shown in Figure 13.

The total masses extracted period by period can be seen in Figure 14.

As can be seen in Figure 14, until the 4th period, the masses moved were very similar in both models. In the 7th period, the drop in extraction in the second approach (Interpolation of specific energy) shown in Figure 14 reinforced the image shown in Figure 10. In total, 118.16 Mt were extracted in the first approach (Interpolation of BWI and Axb) against 102.81 Mt in the second approach (Interpolation of specific energy).

Figures 15 and 16 show the average copper and gold grades, respectively, for both models.

The copper grade restriction in the plant was respected by the software. The copper grade from the 3rd to the 5th period had a different trend; while the average processed copper grade in the second approach increased, that of the first approach reduced. The maximum difference in average copper grade between the models occurred in the 3rd year, being 0.06%. The average gold grade showed tiny differences between the two models, with the maximum difference in the 7th period being 0.05 ppm.

Finally, Figure 17 shows the accumulated NPV for both scenarios.

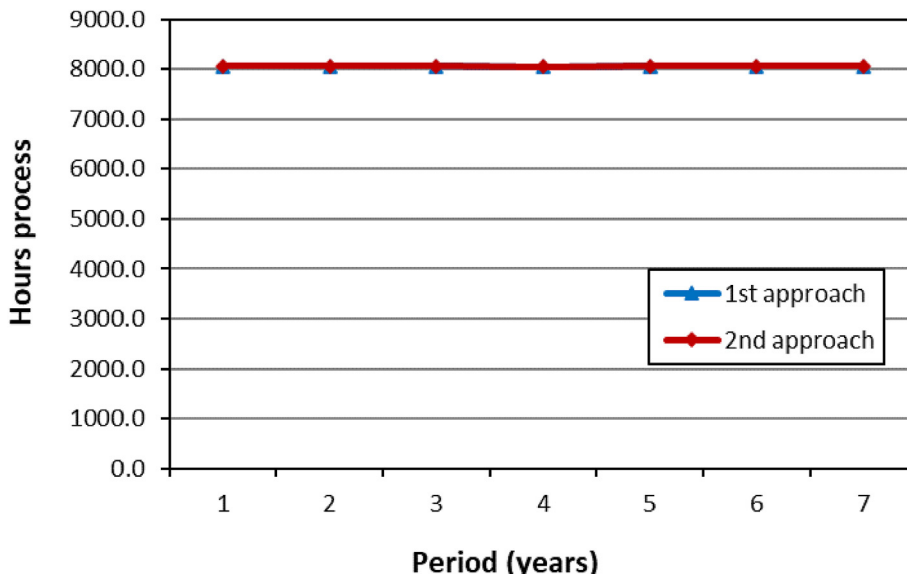


Fig. 13. Annual plant processing time period by period in both approaches (Source: MiningMath).

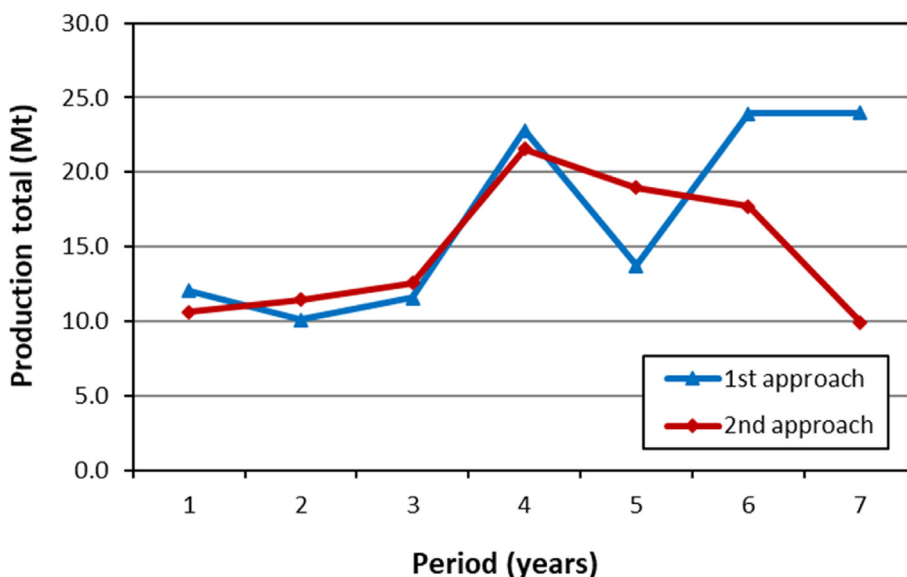


Fig. 14. Total mass extracted period by period in both approaches (Source: MiningMath).

In the first two periods, the accumulated NPV of the model of the second approach (Interpolation of specific energy) was higher, being exceeded from the 3rd period onwards. In the last period, there was an insignificant difference between the two models, with the model of the second approach (Interpolation specific energy) having a higher NPV of 0.54%.

4. Conclusions

This research aimed to verify how the mine scheduling of a real copper and gold mine would be

affected in two different spatial interpolation approaches. In the first approach, the comminution indices Axb and BWI are interpolated to later calculate the specific energy of each block. In the second approach, the specific energy was first calculated from the Axb and BWI data available in the drill holes, and then the specific energy was interpolated in each block. Scheduling optimization using DBS showed:

- Both spatial interpolations returned seven years of life of mine (LoM);

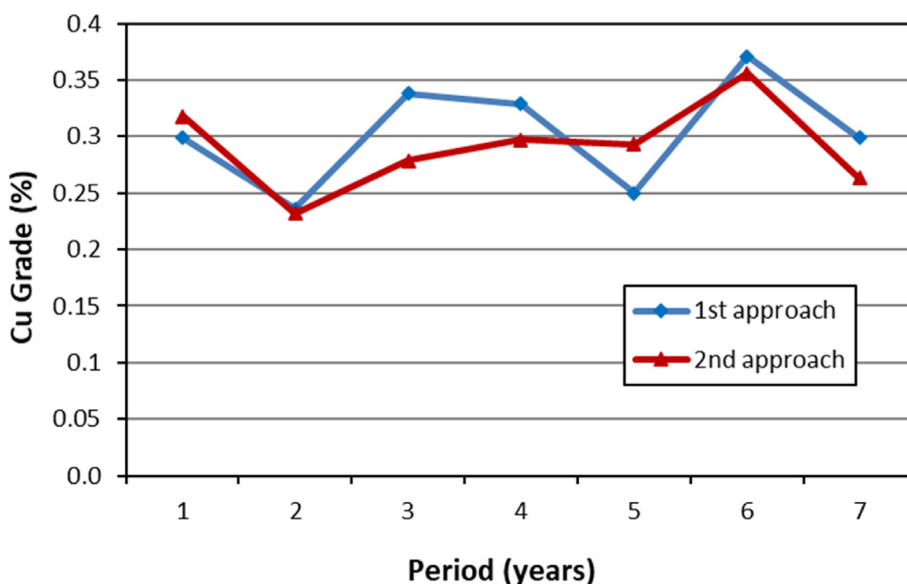


Fig. 15. Average copper grades that fed the process period by period in both approaches (Source: MiningMath).

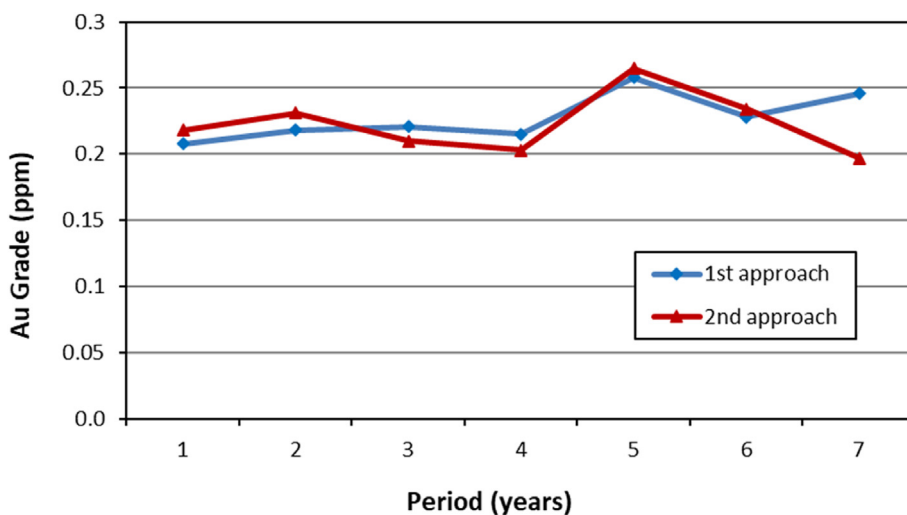


Fig. 16. Average gold grades that fed the process period by period in both approaches (Source: MiningMath).

- Although the block extraction sequence was different in the two approaches, the final pits were similar;
- Both interpolations did not reach the tonnage target due to the plant’s processing hours restriction, with the first approach (Interpolation of BWI and Axb) producing 0.81% more than the second approach (Interpolation of specific energy).
- The first approach (Interpolation of BWI and Axb) produced 4.96% more copper and 2.91% more gold than the second approach (Interpolation of specific energy);

- The accumulated NPV differed between the two methods by only 0.54%.

Therefore, it is concluded that for the case study carried out in this work, the interpolation of comminution indexes returned a mine scheduling similar to the interpolation of specific energy, with similar final pits and similar financial return.

It is important to highlight that it is not possible with this study alone to state that the results will always be similar and it is necessary to evaluate other deposits.

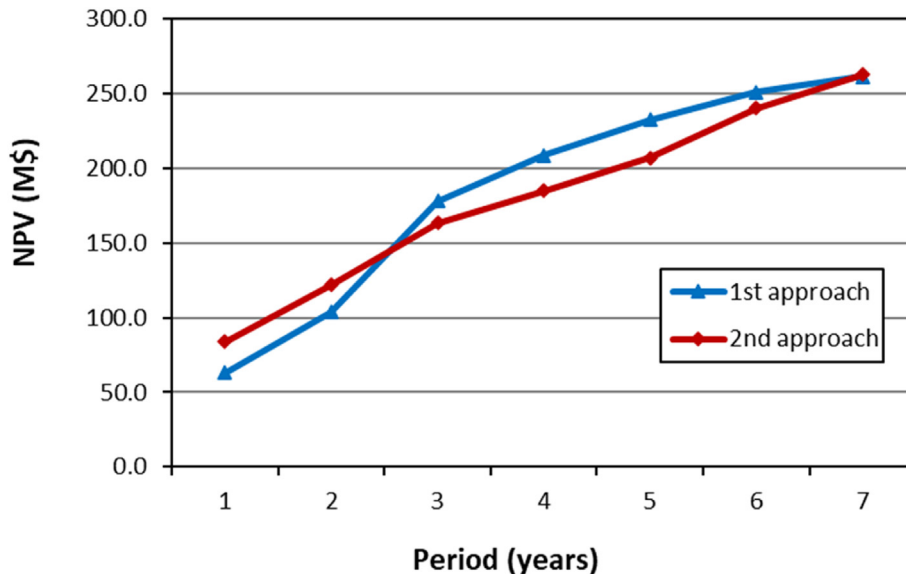


Fig. 17. Cumulative NPV period by period in both approaches (Source: MiningMath).

Ethical statement

The authors state that the research was conducted according to ethical standards.

Funding body

This study was financed in part by the Coordenação de Aperfeiçoamento de Pessoal de Nível Superior - Brasil (CAPES) - Finance Code 001.

Conflicts of interest

The authors declare no conflict of interest.

Acknowledgments

The authors would like to thank MiningMath for the software license provided, the mining company that provided the information necessary to conduct this study, CAPES-PROEX, CNPq and FAPEMIG.

References

- [1] Dominy S, O'Connor L, Parbhakar-Fox A, Glass H, Purevgerel S. Geometallurgy—a route to more resilient mine operations. *Minerals* 2018;8(12):560. <https://doi.org/10.3390/min8120560>.
- [2] Lishchuk V, Koch P, Lund C, Lamberg P. The geometallurgical framework. Malmberget and mikheevskoye case studies. *Min. Sci.* 2015;22(2):57–66. <https://doi.org/10.5277/ms150206>.
- [3] Parian M, Lamberg P, Möckel R, Rosenkranz J. Analysis of mineral grades for geometallurgy: combined element-to-mineral conversion and quantitative X-ray diffraction. *Miner Eng* 2015;82:25–35. <https://doi.org/10.1016/j.mineng.2015.04.023>.
- [4] Garrido M, Sepúlveda E, Ortiz J, Navarro F, Townley B. A methodology for the simulation of synthetic geometallurgical block models of porphyry ore bodies. In: *Proceedings of the Procemin Geomet 2018*. Las Condes; 2018. Santiago.
- [5] Dimitrakopoulos R. *Advances in Applied Strategic Mine planning*. Melbourne: The Australasian Institute of Mining and Metallurgy. 2018.
- [6] Gomes R, Tomi G, Assis P. Mine/Mill production planning based on a Geometallurgical Model. *Rem: Revista Escola de Minas* 2016;69(2):213–8. <https://doi.org/10.1590/0370-44672015690173>.
- [7] Morales N, Seguel S, Caceres A, Jélvez E, Alárcon M. Incorporation of geometallurgical attributes and geological uncertainty into long-term open-pit mine planning. *Minerals* 2019;9(2):108. <https://doi.org/10.3390/min9020108>.
- [8] Alruiz O, Morrell S, Suazo C, Naranjo A. A novel approach to the geometallurgical modelling of the Collahuasi grinding circuit. *Miner Eng* 2009;22(12):1060–7. <https://doi.org/10.1016/j.mineng.2009.03.017>.
- [9] Boisvert J, Rossi M, Ehrig K, Deutsch C. Geometallurgical modeling at olympic dam mine, south Australia. *Math Geosci* 2013;45(8):901–25. <https://doi.org/10.1007/s11004-013-9462-5>.
- [10] Coward S, Vann J, Dunham S, Stewart M. The primary-response framework for geometallurgical variables. In: *Proceedings of the 7th International Mining Geology Conference*; 2009 (paper 17-19). Perth, Western Australia.
- [11] Bond FC. Confirmation of the third theory. In: *Proceedings of the AIME Annual Meeting*; 1959. San Francisco, California.
- [12] JKTech. JK drop Weight tester [internet]. 2023. Retrieved from: <https://jktech.com.au/products/testing-equipment>.
- [13] Global Mining Guidelines Group (GMG). The Morrell Method to determine the efficiency of industrial grinding circuits [internet]. 2021. Retrieved from: https://gmgroup.org/wp-content/uploads/2021/12/GUIDELINE_The-Morrell-Method-to-Determine-the-Efficiency-of-Industrial-Grinding-Circuits_2021.pdf.
- [14] Wills B, Napier-Munn T. *Mineral Processing Technology: an Introduction to the Practical Aspects of Ore Treatment and Mineral*. 7th ed. Oxford, UK: Butterworth-Heinemann; 2006.
- [15] Campos PHA, Costa JFCL, Koppe VC, Bassani MAA. Geometallurgy-oriented mine scheduling considering volume support and non-additivity. *Min Technol* 2021;131(1):1–11. <https://doi.org/10.1080/25726668.2021.1963607>.

- [16] Mata JFC, Nader AS, Mazzinghy DB. Methodology to include the comminution specific energy into open-pit strategy mine planning using global optimization. *TMMM* 2022;19(2752). <https://doi.org/10.4322/2176-1523.20222752>.
- [17] Mata JFC, Nader AS, Mazzinghy DB. Inclusion of the geometallurgical variable specific energy in the mine planning using direct block scheduling. *TMMM* 2022;19(2677). <https://doi.org/10.4322/2176-1523.20222677>.
- [18] Vieira M, Costa J. Geometallurgical modelling to help in predicting zinc metallurgical recovery. In: *Proceedings of the 24th World Mining Congress Proceedings*; 2016 (paper 51-61). Rio de Janeiro, RJ.
- [19] Carrasco P, Chilès J, Séguret SA. Additivity, metallurgical recovery, and grade. In: *Proceedings of the 8th International Geostatistics Congress*; 2008. Santiago, Chile.
- [20] Eivazy H, Esmaili K, Jean R. Challenges in modelling geo-mechanical heterogeneity of rock masses using geostatistical approaches. In: *Proceedings of the 24th World Mining Congress*; 2016 (Paper 27-36). Rio de Janeiro, RJ.
- [21] Campos PHA. Spatial Modeling, Mine Scheduling and Blending Considerations about Geometallurgical Variables. RS, Brazil: Universidade Federal do Rio Grande do Sul; 2023. PhD Thesis.
- [22] Moreira AA, Santos JRGA, Mazzinghy DB. Comportamento geometalúrgico dos índices de cominuição em misturas de diferentes litologias presentes na mina de Chapada. In: *Proceedings of the XXIX Encontro Nacional de Tratamento de Minérios e Metalurgia Extrativa*; 2021. Búzios, RJ.
- [23] Leal RS, Peroni RL, Costa JFCL, Pereira SG, Martins RM, Capponi LN. Geostatistics applied to geometallurgical modeling. In: *Proceedings of the 24th World Mining Congress*; 2016 (paper 115-122). Rio de Janeiro, RJ.
- [24] SMC. SMC masterclass – session 8 - geometallurgical modelling [internet]. 2024. Retrieved from: <https://www.smctesting.com/videos/geometallurgical-geomet-modelling>.
- [25] Campos LJF, Silva PH, Mazzinghy DB, Tavares LM, Campos PHA, Galéry R. Índice de trabalho de bond para moagem de bolas (bwi) é uma variável aditiva?. In: *Proceedings of the XXVIII Encontro Nacional de Tratamento de Minérios e Metalurgia Extrativa*. Belo Horizonte, MG; 2019.
- [26] Bergeron Y, Kojovic T, Gagnon M-d-N, Okono P. Applicability of the HIT for evaluating comminution and geo-mechanical parameters from drill core samples—the Odyssey project case study. In: *Proceedings of the COM 2017*; 2017. Vancouver, Canada.
- [27] Kojovic T. HIT—a portable field device for rapid hardness index testing at site. In: *Proceedings of the AusIMM Mill Operators' Conference 2016*; 2016. paper. 9–16). Perth, Western Australia; 2016.
- [28] Kojovic T, Bergeron Y, Leetmaa K. The value of daily HIT ore hardness testing of SAG feed at the meadowbank gold mine. In: *Proceedings SAG2019*; 2019. Vancouver, Canada.
- [29] Varianemil D, Kojovic T, Hakim D, Dilaga R, Condori P. Ore hardness mapping of Batu Hijau ore deposit using the hardness index tester. In: *Proceedings of the SAG2023*; 2023. Vancouver, Canada.
- [30] Kojovic T, Bergeron Y, Leetmaa K. The value of daily HIT ore hardness testing of SAG feed at the meadowbank gold mine. In: *Proceedings SAG2019*; 2019. Vancouver, Canada.
- [31] Bergeron Y, Kojovic T, Gagnon M-d-N, Okono P. Applicability of the HIT for evaluating comminution and geo-mechanical parameters from drill core samples—the Odyssey project case study. In: *Proceedings of the COM 2017*; 2017. Vancouver, Canada.
- [32] Doll A. SMC Test parameters from A×b. LinkedIn 2024 [internet]. Retrieved from: https://www.linkedin.com/posts/alex-doll-66b57465_comminution-grindability-smctest-activity-7152238024792121344-7hB0.
- [33] Doll A. SMC Test parameters from A×b. LinkedIn 2022 [internet]. Retrieved from: https://www.linkedin.com/posts/alex-doll-66b57465_comminution-grindability-smctest-activity-7152238024792121344-7hB0.
- [34] MiningMath. [internet]. 2022. Retrieved from: <https://knowledge.miningmath.com/general-contents/trending-topics/algorithm-framework>.
- [35] Johnson TB. Optimum Open Pit Mine Production Scheduling. Berkeley, CA, USA: University of California; 1968. PhD Thesis.
- [36] Chicoisne R, Espinoza D, Goycoolea M, Moreno E, Rubio E. A New algorithm for the open-pit mine production scheduling problem. *Oper Res* 2012;60(3):517–28. <https://doi.org/10.1287/opre.1120.1050>. 2012.